

---

# Test-Time Adaptation for Backdoor Defense

---

Jiyang Guan<sup>1,2</sup>, Jian Liang<sup>1,2</sup>, Ran He<sup>1,2</sup>

<sup>1</sup>MAIS & CRIPAC, Institute of Automation, Chinese Academy of Sciences, China

<sup>2</sup>School of Artificial Intelligence, University of Chinese Academy of Sciences, China

guanjiyang2020@ia.ac.cn, liangjian92@gmail.com, rhe@nlpr.ia.ac.cn

## Abstract

Deep neural networks have played a crucial part in many critical domains, such as autonomous driving, face recognition, and medical diagnosis. However, deep neural networks are facing security threats from backdoor attacks and can be manipulated into attacker-decided behaviors by the backdoor attacker. To defend the backdoor, prior research has focused on using clean data to remove backdoor attacks before model deployment. In this paper, we investigate the possibility of defending against backdoor attacks at test time by utilizing partially poisoned data to remove the backdoor from the model. To address the problem, a two-stage method Test-Time Backdoor Defense (TTBD) is proposed. In the first stage, we propose two backdoor sample detection methods, namely DDP and TeCo, to identify poisoned samples from a batch of mixed, partially poisoned samples. Once the poisoned samples are detected, we employ Shapley estimation to calculate the contribution of each neuron's significance in the network, locate the poisoned neurons, and prune them to remove backdoor in the models. Our experiments demonstrate that TTBD removes the backdoor successfully with only a batch of partially poisoned data across different model architectures and datasets against different types of backdoor attacks.

## 1 Introduction

Over the past years, deep neural networks have played a crucial part in many critical domains, such as autonomous driving [1], face recognition [2], and medical diagnosis [3]. Despite their widespread use, deep neural networks lack transparency, making them vulnerable to different attacks. This vulnerability leads to serious mistakes in security-related areas, causing significant threats and concerns. Recent studies have proven that backdoor attacks [4] pose a severe security threat to deep neural networks. Backdoor attacks [5], taking advantage of the overfitting of the deep neural networks, inject the backdoor poisoned data with the small invisible triggers into the model's training dataset, and cause the model trained on that to behave normally on clean samples but predict the wrong, attacker-decided labels on the backdoor poisoned samples. A wide variety of backdoor attacks [5–9] have been proposed, and recent works such as WaNet [9] and LF [8] add invisible backdoor triggers onto clean samples, leading to more serious security threats.

To reduce the threats of backdoor attacks, numerous backdoor defense methods have been proposed, which can generally be classified into two categories: the training stage backdoor defense and the model repairing backdoor defense. Because training deep neural networks is an expensive process that requires significant data collection and computational resources, training on the cloud and directly using third-party well-trained models have become increasingly popular, and thus, in this paper, we mainly focus on the model repairing backdoor defense. The model repairing backdoor defense usually involves retraining [10] or pruning [11, 12] to remove backdoor based on the clean data, for example, by using 5% of clean samples from the training dataset. Previous works have mainly

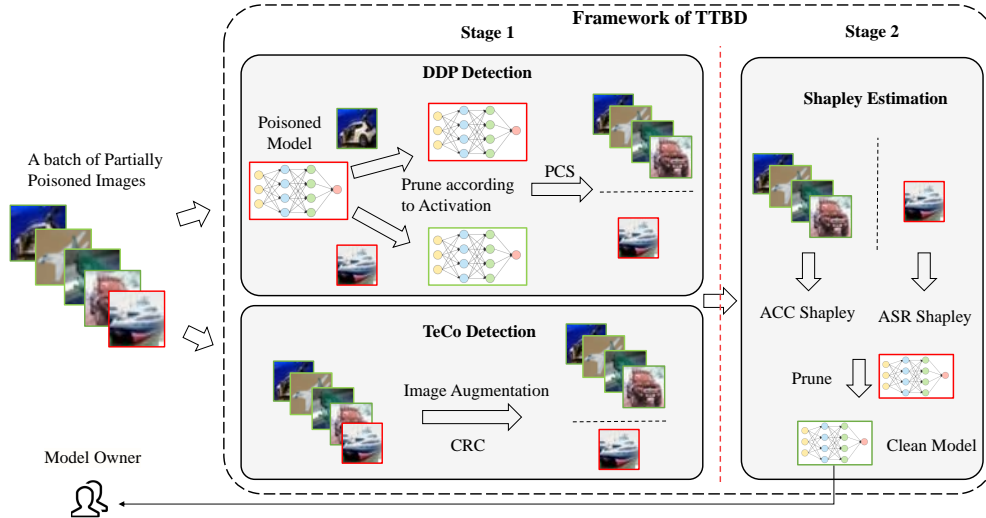


Figure 1: Framework of TTBD. Samples and models in the red broader represent poisoned samples and models, and samples and models in the green broader represent clean samples and models.

focused on repairing poisoned models before model deployment, while in this work, we investigate whether the backdoor defense can be performed during test time by the defender.

At test time, the defenders have access to both the clean samples and the backdoor poisoned samples, or in other words, the partially poisoned data. While the poisoned samples in the mixed, partially poisoned data can help remove backdoor, detecting them accurately poses a significant challenge. Moreover, since poisoned sample detection can not be entirely accurate, there may be some clean samples mixed with the detected poisoned samples, which presents another challenge for backdoor removal. As for the backdoor poisoned sample detection, TeCo [4] is a state-of-the-art backdoor sample detection method that leverages sample corruption robustness consistency to distinguish between poisoned and clean samples. However, TeCo is sensitive to different model architectures and can not successfully distinguish poisoned data from clean data on some model architectures such as VGG [13], causing problems to backdoor removal. To overcome this problem, we propose a novel backdoor detection method called Detection During Pruning (DDP), which can accurately detect poisoned samples across different model architectures. After poisoned data detection, we propose a Shapley-based backdoor cleanse method, which can tolerate imprecise backdoor detection. Our experiments demonstrate that our two-stage test-time backdoor defense framework Test-Time Backdoor Defense (TTBD) can remove backdoor using only a small batch of partially poisoned data (100 images) and remove backdoor in models with only a small decrease in accuracy across different model architectures and datasets facing various types of backdoor attacks.

Our contributions are summarized as follows:

- We propose a novel two-stage test-time backdoor defense framework, TTBD, and reveal that defenders can remove the backdoor at test time with a batch of partially poisoned data.
- We leverage DDP and TeCo to detect the poisoned samples at test time, then use Shapley estimation to guide poisoned neuron pruning and propose two effective test-time backdoor removal methods, TTBD-DDP and TTBD-TeCo.
- The experiments demonstrate that TTBD removes backdoor successfully with only a batch of partially poisoned data across different model architectures and datasets facing various attacks.

## 2 Related Work.

### 2.1 Backdoor Attack

Backdoor attacks, as an important topic in deep neural network security, usually inject poisoned label-flipped samples with the attacker-decided backdoor triggers into the model training dataset and

cause the poisoned model trained on that to behave normally on clean samples but be manipulated on the poisoned samples. The first and most famous backdoor attack is BadNets [5], which injects a small square at the corner of the image as the backdoor trigger, leading to the model’s misclassification on the triggered samples. To make the backdoor trigger more invisible, the following works leverage strategies such as blending [6], natural reflection [14], low frequency [8] and encoder-decoder framework [15] to design the invisible backdoor triggers. Furthermore, to make backdoor attacks more flexible and convert, the multi-target and multi-triggers attacks have been proposed [16, 17].

## 2.2 Backdoor Defense

The backdoor attacks mentioned above pose severe security threats, and a wide range of backdoor defense methods have been proposed. In general, there are two categories of backdoor defense, training stage backdoor defense and model repairing backdoor defense.

**Training Stage Backdoor Defense.** Under this setting, the defenders have access to the training dataset and are able to control the model training process, so that they can detect and filter the poisoned data or add restrictions to suppress the overfitting of backdoor during the training process [17]. The backdoor samples, as outliers of the training dataset, have different representation statics in the feature space and different sensitivity to image transformation, and thus the defenders make use of these differences to filter out the poisoned samples in the training dataset [18, 19]. Other methods leverage restriction to model training to weaken the influence of backdoor samples during training process [20–22].

**Model Repairing Backdoor Defense.** With the rise of machine learning as a service (MLass) in recent years, users can leverage third-party models directly without training models by themselves. However, these models may be poisoned, which poses a significant threat to the users. Under such circumstances, defenders need to remove backdoors from the models without having access to the training dataset or training process. Most model repairing backdoor defense methods leverage clean labeled data to prune backdoor neurons [11, 23], reverse the backdoor trigger and unlearn it [10, 24–26], adversarially activate backdoor neurons [12], and distillate neural attention [27] to remove backdoor. All these methods defend against the backdoor before the model deployment and neglect the backdoor defense during the test-time stage. During test time, the defender can get access to the partially poisoned data and how to use it to remove the backdoor in the deployed models is still a problem. In this paper, we assume the defender can only access a batch of partially poisoned data and remove the backdoor with it.

## 2.3 Test-time Backdoor Defense

There are a few test-time backdoor defense methods [28, 29] having been proposed. However, they focus on either backdoor sample detection [28], or sample-level trigger elimination [29]. Both the backdoor sample detection and the sample-level trigger elimination cause the model to process detection or elimination on each sample and affect the model’s inference speed a lot. Additionally, sample-level trigger elimination requires a pre-trained autoencoder. Since backdoor behavior is typically due to the overfitting of the backdoor triggers and the specific target labels in models, repairing at the model level is generally more effective. Our test-time backdoor defense method removes backdoor attacks by repairing the model using only one batch of partially poisoned samples.

# 3 Proposed Method

## 3.1 Preliminaries

**Problem Definition.** We consider a realistic scenario in which the defender seeks to remove backdoor attacks in models at test time. In this scenario, the attackers attempt to use the poisoned data to attack the defenders’ backdoor models, and intuitively, the defenders are able to make use of those poisoned data to remove the backdoor in their models. However, the attackers typically do not use the fully poisoned data to avoid suspicion of the defenders. Thus in most cases, the defenders are provided partially poisoned data which mixes the clean samples and the poisoned samples. Then how the defenders use the partially poisoned data to remove the backdoor is a challenging problem.

**Defender’s Goals.** The main objective for defenders is to remove backdoor attacks in models while ensuring that clean accuracy is not compromised. Thus, the defenders aim to achieve a model with high accuracy (ACC) and a low attack success rate (ASR).

### 3.2 Poisoned Sample Detection

During test time, the defenders only have access to partially poisoned samples and we hope the defenders remove the backdoor from the models with only a batch of partially poisoned images. To solve the test-time backdoor removal problem, we propose a two-stage backdoor defense method. Intuitively, the first step of backdoor removal is to use poisoned sample detection to distinguish the poisoned samples from clean samples. And then, the defenders leverage these detected poisoned samples to remove the backdoor from the backdoor models. An overview of our framework is shown in Figure 1. In this subsection, we discuss how to distinguish the poisoned samples from the clean ones and propose two poisoned sample detection methods.

**Detection with TeCo.** TeCo [4] is a state-of-the-art backdoor detection method, which utilizes samples’ corruption robustness consistency to distinguish between the poisoned samples and the clean samples. To be specific, TeCo conducts Corruption Robust Consistency (CRC) as the detection indicator. For different corruptions, with corruption’s severity changing, TeCo records the severity at which the images’ prediction changes. Then, TeCo calculates the deviation of recorded severity by different corruptions, expressed as:

$$CRC = deviation(Severity), \quad Severity = [sev_1 \cdots sev_i \cdots sev_n] \quad (1)$$

where  $sev_i$  represents the recorded severity for the  $i$ -th type of corruption. Experiments demonstrate that poisoned samples have a larger CRC than clean samples. Additionally, in most cases, TeCo achieves  $AUC \geq 0.9$ . However, TeCo has some limitations, such as being sensitive to different model architectures. It fails when faced with certain model architectures, such as VGG [13]. To deal with the problem, we propose a new poisoned sample detection method called DDP.

**Detection with DDP.** The previous backdoor detection method TeCo [4] has used the difference in sensitivity between poisoned and clean samples to image transformations as a means of distinguishing between them. According to previous works [11], another difference between poisoned and clean samples is that poisoned samples activate backdoor neurons, while clean samples do not. Therefore, the defenders can make use of the difference in backdoor activation to distinguish the poisoned and clean samples. Pruning neurons with the highest activation value among the poisoned samples will help remove backdoor in models and when the defenders are given a batch of partially poisoned samples, they can use the activation of each sample in the batch to guide the pruning process and remove backdoor attacks in the model. For poisoned samples, pruning neurons with the highest activation value results in a sharp decrease in the model’s ASR, leading to changes in predictions for both normal and poisoned samples. However, for clean samples, pruning neurons with the highest activation value only cause changes in the normal samples. Therefore, we use the prediction change score (PCS) as an indicator of poisoned sample detection. Poisoned samples typically exhibit a higher PCS than clean samples, and PCS is expressed as:

$$PCS = \sum_i (prediction_i \neq \hat{prediction}_i) \quad (2)$$

where  $prediction_i$  represents the original model’s prediction on the  $i$ -th sample and  $\hat{prediction}_i$  represents the pruned model’s prediction on the  $i$ -th sample. To prevent the accuracy of the model from influencing the PCS, pruning is early stopped when the accuracy of the model drops below a certain threshold. Pruning based on samples’ activation value is an intuitive way to remove backdoor in models and detect poisoned samples. However, in our setting, only one sample is used at a time for activation estimation and poisoned neuron location, which reduces the performance of backdoor removal using the poisoned samples’ activation. To address this limitation, we calculate the Shapley value of the neurons using the whole batch of partially poisoned samples as the indicator of neurons which are important to both clean and backdoor samples and prune the neurons with the top- $k$  activation values and the bottom- $l$  Shapley values. This approach provides a more accurate measure of the importance of each neuron in the neural network and can effectively locate the poisoned neurons. The calculation of the Shapley value and its effectiveness will be discussed in Section 3.3.

### 3.3 Backdoor Removal with Shapley Value

Typically, only a small portion of the total neurons in a model act as backdoor neurons, which are activated only when poisoned samples are provided. After pruning these poisoned neurons, the backdoor behavior is removed [11]. Neurons’ activation value is the most commonly used method in locating poisoned neurons and the defenders can prune neurons to remove the backdoor according to their activation value [10, 11]. However, the neuron’s activation value is not accurate and some of the normal neurons also have a larger activation value and it will get worse when the number of samples is small. Thus, it is vital to locate poisoned neurons in a more accurate way. In this subsection, we leverage Shapley value to locate poisoned neurons and remove the backdoor according to it.

**Shapley Value.** In deep neural networks, there are thousands of neurons and complex interactions between them, making it challenging to quantify their contributions to the model’s output. Shapley value, as an important concept in game theory, can allocate each player’s contribution to the outcome [30]. Shapley value is calculated by the average of each player’s marginal value, and Shapley value of player  $i$  is expressed as [31]:

$$\phi_i = \frac{1}{n} \sum_{S \subset N \setminus i} P_S \cdot (V(S \cup i) - V(S)) \quad (3)$$

where  $V$  represents the performance metric,  $N = [1, 2 \dots n]$  represents all  $n$  players,  $S$  represents a subset of  $N$  having  $s$  players, and  $P_S = \frac{(n-s-1)!s!}{(n-1)!}$  represents  $S$ ’s relative importance. In deep neural networks, each player in Equation 3 can be seen as a neuron in the model, and the performance metric  $V$  can be used to represent accuracy (ACC) or attack success rate (ASR) in backdoor defense tasks. Please note that during test time, the partially poisoned samples are unlabeled. To address this issue, our method employs the predicted label of the original model as the label for these samples.

**Estimating Shapley Value.** Because deep neural networks have thousands of neurons, directly calculating Shapley value is time-consuming. To accelerate Shapley calculation, two Shapley estimation acceleration methods are proposed [23, 30]. First is Monte-Carlo estimation. From Equation 3, Shapley value can also be expressed as the average of the marginal value of neurons in all possible orders, expressed as [31]:

$$\phi_i = E_{\pi \in \Pi} (V(S_{\pi}^i \cup i) - V(S_{\pi}^i)) \quad (4)$$

where  $\pi$  represents a random permutation of neurons,  $\Pi$  represents permutation set of all neurons, and  $S_{\pi}^i$  represents neurons after neuron  $i$  in permutation. With Equation 4, we use Monte-Carlo estimation to estimate Shapley value. Furthermore, when pruning neurons during Shapley estimation, models’ ACC and ASR will decrease to near zero after pruning only a small number of neurons, and the marginal values after that are negligible. Thus we can early stop this pruning process to promote estimation efficiency. In our experiments, we set a threshold for model pruning, and if the models’ performance decreases under this threshold, the pruning is early stopped and another new permutation pruning begins. In our experiments, we estimate neurons’ Shapley value with only 40 average iterations, which is accurate enough for locating the poisoned neurons.

**Backdoor Removal.** The Shapley value estimated above indicates the relative importance of neurons to the performance of the model and can be used by defenders to guide neuron pruning. Intuitively, facing the partially poisoned sample situation, the defenders leverage the detected poisoned samples and the labels that the original model predicts to estimate the model’s ASR Shapley value. While the Shapley value is more accurate than model activation, directly pruning the top ASR Shapley value neurons can cause a sharp decrease in accuracy. This is due to the fact that the detected poisoned samples may contain normal samples, and the number of poisoned samples is often small. To address this issue, we estimate the Shapley value of ACC using the entire batch of samples and select neurons with both the top-k ASR Shapley value and the bottom-m ACC Shapley value. Additionally, to prevent neurons from having a small Shapley value due to having both large positive and negative marginal values, we improve Equation 4 and use the mean of the absolute values of the marginal values as the absolute Shapley value, which is expressed as follows:

$$\hat{\phi}_i = E_{\pi \in \Pi} |V(S_{\pi}^i \cup i) - V(S_{\pi}^i)| \quad (5)$$

where  $\hat{\phi}_i$  represents the absolute Shapley value, and  $|\cdot|$  represents the absolute value. Pruning neurons with top-k ASR Shapley value and bottom-m ACC absolute Shapley value, our proposed method locates the poisoned neurons accurately and removes the backdoor with only a small accuracy decrease, only leveraging a batch of partially poisoned data, without the need of fine-tuning the model with clean samples.

## 4 Experiment

### 4.1 Setup

**Datasets and DNNs.** We evaluate various backdoor defense methods on two common datasets used in backdoor defense, CIFAR10 [32] and Tiny-ImageNet [33]. Furthermore, following the BackdoorBench [34], we also evaluate all backdoor defense methods on two common model architectures, PreAct-ResNet18 [35] and VGG19 [13].

**Attack Settings.** We consider 5 popular state-of-the-art backdoor attacks: BadNets [5], Blended [6], SIG [7], LF [8], and WaNet [9]. We follow the default configuration in BackdoorBench [34] for a fair comparison. As for the poisoning rate, to test different defense methods’ performance on different poisoning rates, we set the poisoning rate to 1% for CIFAR10 and 10% for Tiny-ImageNet. To ensure the integrity of our experiments, we set the poisoning rate to 10% for WaNet on CIFAR10 using both PreAct-ResNet and VGG, and for LF on CIFAR10 using VGG, as these attacks are not able to successfully inject a backdoor at 1% poisoning rate (1% poisoning rate injection causes a low ASR). Additionally, since SIG cannot perform an attack on Tiny-ImageNet with poisoning rates of either 1% or 10%, we did not use SIG on Tiny-ImageNet.

**Defense Settings.** Since there have been no prior test-time backdoor defense methods based on model repairing, we compare our method with previous state-of-the-art model-repairing-based backdoor defense methods, including Fine Pruning (FP) [11] and Adversarial Neuron Pruning (ANP) [12]. Additionally, to fully verify the effectiveness of our method, we also include a state-of-the-art training-stage backdoor defense, Decoupling-based Backdoor Defense (DBD) [19]. We follow the default configuration in BackdoorBench [34] for a fair comparison. To ensure the effectiveness of the compared backdoor defense methods, following BackdoorBench, we have specified that FP and ANP have access to 5% of the benign training data, and DBD can access the full poisoned training dataset and control model’s training process. Additionally, we set the partially poisoned data’s poisoning rate to 10% in our test-time backdoor defense setting, and the image batch used in TTBD only consists of 100 partially poisoned samples. Furthermore, we study the influence of the poisoning rates and the batch sizes on our TTBD’s performance in Section 4.3. Additionally, for poisoned sample detection, we have selected the top 10 detected samples in TeCo and the top 6 detected samples in DDP as our identified poisoned samples. We have used these samples to estimate the ASR Shapley value of neurons and remove the backdoor in the models.

**Evaluation Metric.** We use two commonly used metrics to measure the effectiveness of different backdoor defense methods: accuracy on clean samples (ACC) and attack success rate on poisoned samples (ASR). The ultimate goal of defenders is to leverage various methods to achieve a no-backdoor model with high ACC and low ASR.

### 4.2 Experiment Results

Table 1: Different defense methods against common attacks on PreAct-ResNet18 using CIFAR10.

Attack (%)	Before		FP[11]		ANP [12]		DBD [19]		TTBD-TeCo		TTBD-DDP	
	ACC	ASR	ACC $\uparrow$	ASR $\downarrow$	ACC $\uparrow$	ASR $\downarrow$	ACC $\uparrow$	ASR $\downarrow$	ACC $\uparrow$	ASR $\downarrow$	ACC $\uparrow$	ASR $\downarrow$
BadNet [5]	91.23	90.22	91.58	51.52	86.09	1.79	78.09	2.99	88.57	1.17	88.50	2.51
Blended [6]	93.76	94.88	93.48	94.14	86.92	37.01	70.18	8.04	86.00	3.00	88.53	2.24
SIG [7]	91.45	91.47	92.17	94.57	86.26	25.04	75.01	67.82	88.42	2.17	89.59	2.77
LF [8]	93.76	86.74	93.30	87.37	84.76	17.78	79.13	7.47	90.28	2.05	90.47	2.72
WaNet [9]	91.48	89.91	91.55	0.20	88.36	0.66	80.90	6.61	91.58	0.49	91.07	0.78
Average	92.34	90.64	92.42	65.56	86.48	16.46	76.66	18.59	88.97	1.78	89.63	2.20

Table 2: Different defense methods against common attacks on VGG19 using CIFAR10.

Attack (%)	Before		FP[11]		ANP [12]		DBD [19]		TTBD-TeCo		TTBD-DDP	
	ACC	ASR	ACC $\uparrow$	ASR $\downarrow$	ACC $\uparrow$	ASR $\downarrow$	ACC $\uparrow$	ASR $\downarrow$	ACC $\uparrow$	ASR $\downarrow$	ACC $\uparrow$	ASR $\downarrow$
BadNet [5]	90.53	84.45	90.35	79.58	-	-	10.00	100.00	88.50	84.97	87.11	1.63
Blended [6]	90.81	88.31	90.62	87.90	-	-	10.00	0.00	86.78	89.73	86.97	4.81
SIG [7]	90.75	82.93	90.60	83.46	-	-	10.00	0.00	88.38	83.95	89.48	2.64
LF [8]	88.88	93.43	88.79	92.39	-	-	10.00	100.00	86.61	88.18	87.04	1.68
WaNet [9]	89.29	85.63	89.67	72.07	-	-	10.00	100.00	88.24	1.38	88.58	1.82
Average	90.05	86.95	90.01	83.08	-	-	10.00	60.00	87.70	69.64	87.84	2.52

Table 3: Different defense methods against common attacks on PreAct-ResNet18 using Tiny-ImageNet.

Attack (%)	Before		FP[11]		ANP [12]		DBD [19]		TTBD-TeCo		TTBD-DDP	
	ACC	ASR	ACC $\uparrow$	ASR $\downarrow$	ACC $\uparrow$	ASR $\downarrow$	ACC $\uparrow$	ASR $\downarrow$	ACC $\uparrow$	ASR $\downarrow$	ACC $\uparrow$	ASR $\downarrow$
BadNet [5]	55.17	99.91	50.13	99.86	49.83	0.07	44.12	98.89	49.42	2.83	53.24	0.25
Blended [6]	55.03	99.78	49.75	99.39	50.38	96.02	44.51	100.00	47.86	3.75	48.92	7.89
LF [8]	54.93	98.91	50.37	98.26	49.48	94.44	43.80	98.67	51.43	1.81	50.51	0.77
WaNet [9]	46.98	98.00	48.35	73.03	44.98	1.36	44.00	99.71	46.92	0.48	47.00	0.60
Average	53.03	99.15	49.65	92.64	48.67	47.97	44.11	99.32	48.91	2.22	49.92	2.38

Tables 1, 2, and 3 demonstrate the performance of TTBD-TeCo and TTBD-DDP across different model architectures (PreAct-ResNet18 and VGG19) and datasets (CIFAR10 and Tiny-ImageNet), as evaluated against 5 different state-of-the backdoor attacks. Before represents the original backdoor model without model defense mechanisms, while FP, ANP, DBD, TTBD-TeCo, and TTBD-DDP represent the repaired model with the specific backdoor defense. In most cases, our TTBD backdoor defense methods remove backdoor in models with a small decline in accuracy (around 2% average accuracy decline on CIFAR10). In Table 2, because ANP can not work on VGG, we use '-' to fill in the blank. Additionally, since SIG cannot perform an attack on Tiny-ImageNet with poisoning rates of either 1% or 10%, we did not use SIG on Tiny-ImageNet. Due to the possibility of detection errors in some samples during TeCo and DDP, a small percentage of poisoned samples may be mistakenly identified as clean samples. This makes it difficult for the defender to fine-tune the model using the detected clean samples directly, as the presence of even a very small percentage of poisoned samples can lead to the backdoor being retained in the model. Typically, most previous model repairing backdoor defense methods need clean samples to fine-tune the backdoor model and maintain the models' accuracy. Although without clean samples to fine-tune the model, our TTBD-TeCo and TTBD-DDP can effectively remove the backdoor by pruning a small percentage of neurons, and our backdoor removal procedure removes the backdoor (using top-k ASR Shapley values) with a small decline in accuracy (using bottom-m ACC absolute Shapley values). In Table 3, there is a slightly greater decrease in accuracy on Tiny-ImageNet by our TTBD-based methods compared with the results on CIFAR10. This is due to the lack of fine-tuning with clean data, as models trained on Tiny-ImageNet have fewer redundant neurons than models trained on CIFAR10. And if the defender can obtain access to some clean samples for fine-tuning, the accuracy of the models can be recovered.

While TTBD-TeCo and TTBD-DDP yield comparable backdoor defense results on PreAct-ResNet using both CIFAR10 and Tiny-ImageNet, TTBD-TeCo is not effective on VGG models. This is because TeCo's detection is sensitive to variations in model architectures, resulting in an AUC of approximately 0.5 on VGG models. In contrast, TTBD-DDP successfully removes backdoor attacks across various model architectures and datasets. Figure 2 demonstrates the change in ACC and ASR of TTBD-DDP and TTBD-TeCo during the pruning of neurons on VGG19 models using the CIFAR10 dataset, where red lines represent ASR and blue lines represent ACC. In most cases, 5 backdoor attacks are removed by pruning only 1% neurons under our TTBD backdoor defense methods. With that small number of neurons being pruned, TTBD does not need clean samples to fine-tune the model and overcome the possible problem of poisoned samples mixed in the detected clean samples. On VGG19, because TeCo can not accurately detect the poisoned samples, TTBD-TeCo fails against most of the attacks and only remove the WaNet attack. While, in most cases in Tables 1 and 3, TTBD-TeCo can also remove backdoor with pruning around 1% of the model's total neurons.

On the other hand, the compared methods have their weaknesses and are not as successful in removing backdoor attacks from models. For instance, FP [11] fails because neuron activation is not

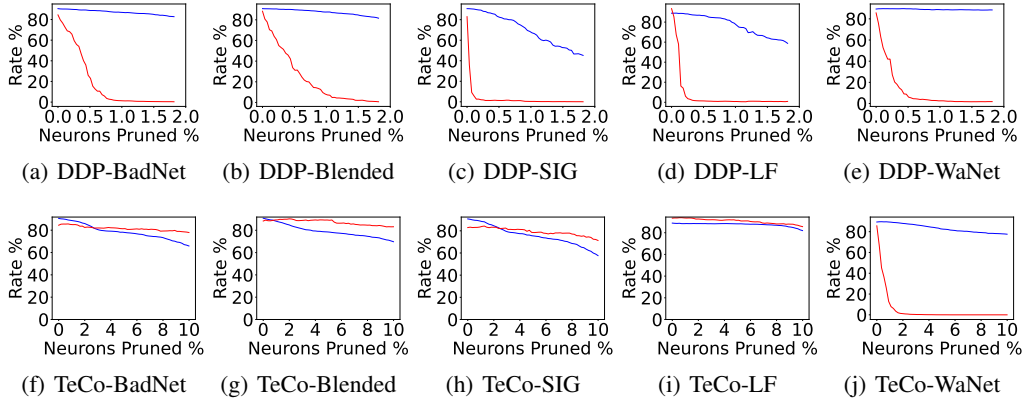


Figure 2: TTBD’s performance against different attacks on VGG19.

an accurate way to identify the poisoned neurons. As a result, pruning neurons based on the smallest activation is unable to pinpoint and eliminate the poisoned neurons responsible for the backdoor attack. Additionally, ANP [12] leverages neurons which are sensitive to adversarial training and masks them, but this approach leads to significant accuracy reductions in the models. DBD [19] leverages self-supervised learning to train backbone models, train the fully connected layers, and removes labels of low-credit samples to fine-tune the source models. Table 1 demonstrates that while DBD is able to remove backdoors from the models, the accuracy of the resulting models is significantly lower than the accuracy of the original backdoor models. In comparison, TTBD-DDP reduces the backdoor to an average ASR of 2.20% with only a 2.71% accuracy decrease, and TTBD-TeCo reduces the backdoor to an average ASR of 1.78% with only a 3.37% accuracy decrease on PreAct-ResNet18 using CIFAR10. Importantly, both TTBD-TeCo and TTBD-DDP are capable of removing backdoor attacks from models with only a small batch of 100 partially poisoned samples, thus highlighting their effectiveness in real-world scenarios.

### 4.3 Influence on Different Poisoning Rates and Batch Sizes

Table 4: TTBD-DDP’s performance with different poisoning rates.

Attack (%)	Before		FP[11]		DBD [19]		TTBD-0.05		TTBD-0.10		TTBD-0.20	
	ACC	ASR	ACC $\uparrow$	ASR $\downarrow$	ACC $\uparrow$	ASR $\downarrow$	ACC $\uparrow$	ASR $\downarrow$	ACC $\uparrow$	ASR $\downarrow$	ACC $\uparrow$	ASR $\downarrow$
BadNet [5]	90.53	84.45	90.35	79.58	10.00	100.00	84.67	3.68	87.11	1.63	88.30	1.60
Blended [6]	90.81	88.31	90.62	87.90	10.00	0.00	82.34	5.96	86.97	4.81	85.32	1.94
SIG [7]	90.75	82.93	90.60	83.46	10.00	0.00	88.61	0.99	89.48	2.64	89.23	0.98
LF [8]	88.88	93.43	88.79	92.39	10.00	100.00	88.02	2.28	87.04	1.68	88.18	1.92
WaNet [9]	89.29	85.63	89.67	72.07	10.00	100.00	88.35	3.54	88.58	1.82	88.47	1.46
Average	90.05	86.95	90.01	83.08	10.00	60.00	86.40	3.29	87.84	2.52	87.90	1.58

Table 5: TTBD-DDP’s performance with different batch sizes.

Attack (%)	Before		FP[11]		DBD [19]		TTBD-50		TTBD-100		TTBD-200	
	ACC	ASR	ACC $\uparrow$	ASR $\downarrow$	ACC $\uparrow$	ASR $\downarrow$	ACC $\uparrow$	ASR $\downarrow$	ACC $\uparrow$	ASR $\downarrow$	ACC $\uparrow$	ASR $\downarrow$
BadNet [5]	90.53	84.45	90.35	79.58	10.00	100.00	85.30	1.24	87.11	1.63	88.42	1.26
Blended [6]	90.81	88.31	90.62	87.90	10.00	0.00	86.07	4.40	86.97	4.81	87.09	2.95
SIG [7]	90.75	82.93	90.60	83.46	10.00	0.00	88.68	1.87	89.48	2.64	89.50	1.00
LF [8]	88.88	93.43	88.79	92.39	10.00	100.00	87.42	2.21	87.04	1.68	87.73	2.82
WaNet [9]	89.29	85.63	89.67	72.07	10.00	100.00	86.77	5.44	88.58	1.82	87.69	2.53
Average	90.05	86.95	90.01	83.08	10.00	60.00	86.85	3.03	87.84	2.52	88.09	2.11

In this subsection, we analyze the influence of different poisoning rates and batch sizes on TTBD-DDP on VGG19 using CIFAR10. Table 4 demonstrates TTBD-DDP’s performance across different poisoning rates of the partially poisoned image batch. Specifically, TTBD-0.05, TTBD-0.10, and



TTBD-0.20 represent TTBD-DDP’s performance using the image batch with 5%, 10%, and 20% poisoning rates, respectively, with the batch size of 100. With the increase of the poisoning rates, TTBD-DDP’s performance rises. TTBD-DDP can remove all of the five types of backdoor attacks with only 5% poisoning rate, and under this poisoning rate, TTBD-DDP achieves an average  $ASR = 3.29\%$  with a 3.65% accuracy loss. Although it’s lower than TTBD-DDP with 10% poisoning rate, it’s still more effective than FP [11] or DBD [19], which can not remove the backdoor on VGG19. Furthermore, under 10% and 20% poisoning rates, all of the five backdoor attacks are removed from the model with a small accuracy decline. Table 5 demonstrates TTBD-DDP’s performance across different batch sizes of the image batch, where TTBD-50, TTBD-100, and TTBD-200 represent TTBD-DDP’s performance using 50, 100, 200 partially poisoned samples with the poisoning rate of 10%. With the increase of the batch sizes, TTBD-DDP’s performance rises and TTBD-DDP can remove all the five backdoor attacks with only 50 partially poisoned samples.

#### 4.4 Ablation Study

Table 6: Ablation Study against five common attacks on PreAct-ResNet18 using CIFAR10.

Attack (%)	Before		TTBD-random		TTBD-activation		TTBD-TeCo		TTBD-DDP	
	ACC	ASR	ACC↑	ASR↓	ACC↑	ASR↓	ACC↑	ASR↓	ACC↑	ASR↓
BadNet [5]	91.23	90.22	82.30	10.90	88.58	51.53	88.57	1.17	88.50	2.51
Blended [6]	93.76	94.88	85.29	92.90	88.65	3.28	86.00	3.00	88.53	2.24
SIG [7]	91.45	91.47	82.92	81.08	83.30	18.10	88.42	2.17	89.59	2.77
LF [8]	93.76	86.74	85.56	91.88	85.32	35.74	90.28	2.05	90.47	2.72
WaNet [9]	91.48	89.91	83.21	78.78	91.02	0.50	91.58	0.49	91.07	0.78
Average	92.34	90.64	83.86	71.11	87.37	21.83	88.97	1.78	89.63	2.20

In this subsection, we will take poisoned sample detection and backdoor neuron locating into consideration to validate our method’s effectiveness. In Table 6, TTBD-random represents randomly selecting samples from the partially poisoned samples and using Shapley estimation to prune the poisoned neurons, and TTBD-activation represents leveraging samples detected by DDP and using neurons’ activation to locate poisoned neurons. Randomly chosen samples are not relevant to the backdoor behavior, and thus, the models after TTBD-random have an average 19.53% ASR decrease but also have an average 8.48% ACC decrease. Additionally, due to the fact that neurons’ activation on poisoned samples does not directly correspond to their importance in terms of ASR, the TTBD-activation approach exhibits a lower ACC-ASR compared to TTBD-TeCo and TTBD-DDP when facing different types of attacks. Moreover, the presence of clean samples mixed in with the detected poisoned samples and the limited number of detected samples present challenges for TTBD-activation. As a result of these factors, TTBD-activation is unable to completely remove the backdoor effect in the models, and the average ASR remains at 21.83%.

## 5 Conclusion and Limitation

This paper introduces a test-time backdoor defense framework called TTBD, which leverages a two-stage framework to detect and remove the backdoor from the poisoned models with only a batch of partially poisoned samples. To detect the poisoned samples from the partially poisoned data, two backdoor sample detection methods DDP and TeCo are proposed. DDP leverages the prediction changes during pruning to accurately detect poisoned samples. After poisoned sample detection, we leverage Shapley estimation to prune the backdoor-related neurons. Using the TTBD framework, two methods, TTBD-DDP and TTBD-TeCo, successfully remove five state-of-the-art backdoor attacks using only a batch of partially poisoned data across different model architectures and datasets. Furthermore, TTBD demonstrates the ability to remove backdoor in models with varying batch sizes or poisoning rates. Considering that the performance of TTBD is influenced by the accuracy of poisoned sample detection, and both DDP and TeCo can be further improved, our future research will focus on developing more precise methods for detecting poisoned samples.

## 6 Broader Impact

TTBD effectively removes various backdoor attacks in models across diverse datasets and model architectures during test-time evaluation. However, backdoor defense may be applied in some areas, such as cleansing of the model watermark, and may cause some problems in model IP protection.

### References

- [1] Yuchi Tian, Kexin Pei, Suman Jana, and Baishakhi Ray. Deeptest: Automated testing of deep-neural-network-driven autonomous cars. In *Proc. SEC*, pages 303–314, 2018.
- [2] Yaniv Taigman, Ming Yang, Marc’Aurelio Ranzato, and Lior Wolf. Deepface: Closing the gap to human-level performance in face verification. In *Proc. CVPR*, pages 1701–1708, 2014.
- [3] Daniel S Kermany, Michael Goldbaum, Wenjia Cai, Carolina CS Valentim, Huiying Liang, Sally L Baxter, Alex McKeown, Ge Yang, Xiaokang Wu, Fangbing Yan, et al. Identifying medical diagnoses and treatable diseases by image-based deep learning. *Cell*, 172(5):1122–1131, 2018.
- [4] Xiaogeng Liu, Minghui Li, Haoyu Wang, Shengshan Hu, Dengpan Ye, Hai Jin, Libing Wu, and Chaowei Xiao. Detecting backdoors during the inference stage based on corruption robustness consistency. In *Proc. CVPR*, 2023.
- [5] Tianyu Gu, Brendan Dolan-Gavitt, and Siddharth Garg. Badnets: Identifying vulnerabilities in the machine learning model supply chain. *arXiv preprint arXiv:1708.06733*, 2017.
- [6] Xinyun Chen, Chang Liu, Bo Li, Kimberly Lu, and Dawn Song. Targeted backdoor attacks on deep learning systems using data poisoning. *arXiv preprint arXiv:1712.05526*, 2017.
- [7] Mauro Barni, Kassem Kallas, and Benedetta Tondi. A new backdoor attack in cnns by training set corruption without label poisoning. In *Proc. ICIP*, pages 101–105. IEEE, 2019.
- [8] Yi Zeng, Won Park, Z Morley Mao, and Ruoxi Jia. Rethinking the backdoor attacks’ triggers: A frequency perspective. In *Proc. ICCV*, pages 16473–16481, 2021.
- [9] Anh Nguyen and Anh Tran. Wanet–imperceptible warping-based backdoor attack. In *Proc. ICLR*, 2021.
- [10] Bolun Wang, Yuanshun Yao, Shawn Shan, Huiying Li, Bimal Viswanath, Haitao Zheng, and Ben Y Zhao. Neural cleanse: Identifying and mitigating backdoor attacks in neural networks. In *Proc. SP*, pages 707–723. IEEE, 2019.
- [11] Kang Liu, Brendan Dolan-Gavitt, and Siddharth Garg. Fine-pruning: Defending against backdooring attacks on deep neural networks. In *Proc. RAID*, pages 273–294, 2018.
- [12] Dongxian Wu and Yisen Wang. Adversarial neuron pruning purifies backdoored deep models. In *Badnets: Identifying vulnerabilities in the machine learning model supply chain*, pages 16913–16925, 2021.
- [13] Karen Simonyan and Andrew Zisserman. Very deep convolutional networks for large-scale image recognition. *arXiv preprint arXiv:1409.1556*, 2014.
- [14] Yunfei Liu, Xingjun Ma, James Bailey, and Feng Lu. Reflection backdoor: A natural backdoor attack on deep neural networks. In *Proc. ECCV*, pages 182–199. Springer, 2020.
- [15] Yuezun Li, Yiming Li, Baoyuan Wu, Longkang Li, Ran He, and Siwei Lyu. Invisible backdoor attack with sample-specific triggers. In *Proc. ICCV*, pages 16463–16472, 2021.
- [16] Mingfu Xue, Can He, Jian Wang, and Weiqiang Liu. One-to-n & n-to-one: Two advanced backdoor attacks against deep learning models. *IEEE Transactions on Dependable and Secure Computing*, 19(3):1562–1578, 2020.
- [17] Runkai Zheng, Rongjun Tang, Jianze Li, and Li Liu. Pre-activation distributions expose backdoor neurons. *Proc. NeurIPS*, pages 18667–18680, 2022.

- [18] Bao Gia Doan, Ehsan Abbasnejad, and Damith C Ranasinghe. Februus: Input purification defense against trojan attacks on deep neural network systems. In *Proc. ACSAC*, pages 897–912, 2020.
- [19] Kunzhe Huang, Yiming Li, Baoyuan Wu, Zhan Qin, and Kui Ren. Backdoor defense via decoupling the training process. In *Proc. ICLR*, 2022.
- [20] Yige Li, Xixiang Lyu, Nodens Koren, Lingjuan Lyu, Bo Li, and Xingjun Ma. Anti-backdoor learning: Training clean models on poisoned data. In *Proc. NeurIPS*, pages 14900–14912, 2021.
- [21] Elan Rosenfeld, Ezra Winston, Pradeep Ravikumar, and Zico Kolter. Certified robustness to label-flipping attacks via randomized smoothing. In *Proc. ICML*, pages 8230–8241, 2020.
- [22] Jacob Steinhardt, Pang Wei Koh, and Percy Liang. Certified defenses for data poisoning attacks. In *Proc. NeurIPS*, 2017.
- [23] Jiyang Guan, Zhuozhuo Tu, Ran He, and Dacheng Tao. Few-shot backdoor defense using shapley estimation. In *Proc. CVPR*, pages 13358–13367, 2022.
- [24] Liuwan Zhu, Rui Ning, Cong Wang, Chunsheng Xin, and Hongyi Wu. Gangsweep: Sweep out neural backdoors by gan. In *Proc. ACM MM*, pages 3173–3181, 2020.
- [25] Wenbo Guo, Lun Wang, Yan Xu, Xinyu Xing, Min Du, and Dawn Song. Towards inspecting and eliminating trojan backdoors in deep neural networks. In *Proc. ICDM*, pages 162–171, 2020.
- [26] Huili Chen, Cheng Fu, Jishen Zhao, and Farinaz Koushanfar. Deepinspect: A black-box trojan detection and mitigation framework for deep neural networks. In *Proc. IJCAI*, 2019.
- [27] Yige Li, Xixiang Lyu, Nodens Koren, Lingjuan Lyu, Bo Li, and Xingjun Ma. Neural attention distillation: Erasing backdoor triggers from deep neural networks. In *Proc. ICLR*, 2021.
- [28] Xi Li, Zhen Xiang, David J Miller, and George Kesidis. Test-time detection of backdoor triggers for poisoned deep neural networks. In *Proc. ICASSP*, pages 3333–3337. IEEE, 2022.
- [29] Tao Sun, Lu Pang, Chao Chen, and Haibin Ling. Mask and restore: Blind backdoor defense at test time with masked autoencoder. *arXiv preprint arXiv:2303.15564*, 2023.
- [30] Amirata Ghorbani and James Zou. Neuron shapley: Discovering the responsible neurons. In *Proc. ICLR*, 2020.
- [31] Javier Castro, Daniel Gómez, and Juan Tejada. Polynomial calculation of the shapley value based on sampling. *Computers & Operations Research*, 36(5):1726–1730, 2009.
- [32] Alex Krizhevsky, Geoffrey Hinton, et al. Learning multiple layers of features from tiny images. 2009.
- [33] Ya Le and Xuan Yang. Tiny imagenet visual recognition challenge. *CS 231N*, 7(7):3, 2015.
- [34] Baoyuan Wu, Hongrui Chen, Mingda Zhang, Zihao Zhu, Shaokui Wei, Danni Yuan, and Chao Shen. Backdoorbench: A comprehensive benchmark of backdoor learning. In *Proc. NeurIPS*, pages 10546–10559, 2022.
- [35] Kaiming He, Xiangyu Zhang, Shaoqing Ren, and Jian Sun. Identity mappings in deep residual networks. In *Proc. ECCV*, pages 630–645. Springer, 2016.